

Vertical Land Motion from present-day deglaciation in the wider Arctic

Carsten Ankjær Ludwigsen¹, Shfaqat Abbas Khan¹, Ben Marzeion² and Ole Baltazar Andersen¹

¹DTU Space, Technical University of Denmark

²Institute of Geography and MARUM – Center for Marine Environmental Sciences, University of Bremen, Germany

Key Points:

- Elastic VLM caused by present-day melt of Greenland causes significant uplift of coastlines in North America and Northern Europe.
- A VLM-model combining GIA and the elastic rebound from present-day ice loss yields good agreement with GNSS-stations in the wider Arctic.
- Residuals between GNSS and modeled VLM can quantify local circumstances causing VLM.

Corresponding author: Carsten Ankjær Ludwigsen, caanlu@space.dtu.dk

Abstract

Vertical land motion (VLM) of Earth's surface can aggravate or mitigate ongoing relative sea level change. The near-linear process of Glacial Isostatic Adjustment (GIA) is normally assumed to govern regional VLM. However, present-day deglaciation of primarily the Greenland Ice Sheet causes a significant non-linear elastic uplift of $>1 \text{ mm yr}^{-1}$ in most of the wider Arctic. The elastic VLM exceeds GIA at 14 of 42 Arctic GNSS-sites, including sites in non-glaciated areas in the North Sea region and along the east coast of North America. The combined elastic VLM + GIA model is consistent with measured VLM at three-fourth of the GNSS-sites ($R=0.74$), which outperforms a GIA-only model ($R=0.60$). Deviations from GNSS-measured VLM, are interpreted as estimates of local circumstances causing VLM. Future accelerated ice loss on Greenland, will increase the significance of elastic uplift for North America and Northern Europe and become important for coastal sea level projections.

Plain Language Summary

From 2003 to 2015, the Northern Hemisphere lost more than 6000 gigatonnes of ice, contributing with nearly 17 mm to the global mean sea level rise. Loss of land-based ice results in a vertical deformation of the Earth's surface. An ongoing rebound or subsidence caused by the end of the last ice age is often assumed to govern the vertical deformation. But also present-day ice loss from Greenland and Arctic glaciers cause an immediate vertical deformation. By using a vertical deformation model, that includes both components, we can explain GPS-measured deformation in the entire Arctic. Our results show, that the present-day Arctic ice loss contribution to vertical deformation is an uplift in the order 0.5 to 1 mm/yr in a wider northern region. This exceeds the deformation caused by the disappearance of the last ice ages at many coastal regions, including the North Sea region and along the North American Atlantic coast. The present-day ice loss included in the VLM-model equals a global sea level rise of 1.4 mm/yr. This means that 30-80% of the sea level rise caused by Arctic ice loss is mitigated by an surface uplift caused by the same ice loss.

1 Introduction

The Arctic region is warming faster than any other region on Earth (Post et al., 2019). Deglaciation of Arctic land-based ice accounts for 70 % of the total barysteric contribution to sea level rise (Abram et al., 2019) and has over the last 3 decades accelerated the sea level rise with 0.035 mm yr^{-1} (Nerem et al., 2018) every year. From 2003 to 2015 the Greenland Ice Sheet and adjoining glaciers contributed in total with 1 cm of sea level rise while other Arctic glaciers contributed with 0.8 cm (Zemp et al., 2019).

Deglaciation of land ice is also changing the spatial pattern of sea level change. One effect of the redistribution of mass from ice to ocean is the gravitational change (Bamber & Riva, 2010; Hsu & Velicogna, 2017; Adhikari et al., 2019), and influx of freshwater changing the steric sea surface height (Ludwigsen & Andersen, 2020; Armitage et al., 2020). A more overlooked outcome of present-day deglaciation is vertical land motion (Riva et al., 2017). Vertical Land Motion (VLM) has to be taken into account and corrected for, when studying sea level change based on tide gauges (Watson et al., 2015; Wöppelmann & Marcos, 2016). Coastal uplift can mitigate the increasing risk of coastal flooding, while subsidence will aggravate the hazards caused by rising sea levels.

VLM is a composite of multiple ongoing processes, with the viscoelastic relaxation of the Earth's surface since the ending of the last ice ages 21 kyr ago, also known as Glacial Isostatic Adjustment (GIA), being the most prominent component (Farrell & Clark, 1976; Tushingham & Peltier, 1991; Milne & Mitrovica, 1998; Peltier et al., 2015). In general, studies of coastal sea level change, only consider GIA (Church & White, 2011; Jevrejeva et al., 2014), while the elastic contribution is oftentimes ignored.

The physics of the immediate elastic surface response to the changing ice load is well known (Farrell, 1972), and can be used as a proxy for studying glacial ice mass balance (Khan et al., 2010, 2016). Locally, hydrology, tectonics and other seismic effects like earthquakes can be the single largest contribution to VLM (Klos et al., 2019) SLANGEN ref?.

While GIA is dominant in non-glaciated regions, GIA alone is insufficient to explain the measured VLM in the Arctic (Henry et al., 2012). We show, that the elastic VLM in the wider Arctic (roughly defined as the region above 50° latitude) caused by Arctic ice loss since 2003 is significant. The elastic VLM is for most of the region, including the North American coastlines and northern Europe, within the same magnitude as the corresponding barystatic sea level change.

2 Data and Method

Commonly, gravimetric ice mass change data from GRACE (The Gravity Recovery and Climate Experiment) is used to estimate surface loading (Adhikari et al., 2016; Riva et al., 2017; Frederikse et al., 2019). GRACE is convenient because it 'weighs' the Earth, and easily detects changes over time. The spatial signal wavelength of 300-500 km of GRACE is, however, insufficient to reproduce realistic elastic VLM-signals in the proximity of glaciers and ice sheets. Instead, we use mass balance data from Arctic glaciers and Greenland, to create an yearly ice-model with a $2 \times 2 \text{ km}$ spatial resolution from 2003-2015 (see section 2.1).

The ice-model surface loading is used as input for the REAR (Regional ELastic Rebound calculator), (Melini et al., 2014, 2015) to make an elastic VLM-model with the same, high resolution ($2 \times 2 \text{ km}$). REAR is build on the sea level equation of Farrell and Clark (1976) and assumes a solid, non-rotating and isotropic earth. By combining GIA with the elastic VLM model, the VLM-model can be evaluated against GNSS measurements.

The calculated temporal average elastic VLM-rate from 2003-2015 is shown in figure 1. Yearly averaged mass balance changes of glaciers and the Greenland Ice Sheet (see section 2.1) from 2003-2015 are converted to elevation change assuming uniform ice density of 917 kg m^{-3} . The spatial resolution of the ice loading, used as input, and elastic VLM output is $2 \times 2 \text{ km}$, allowing us to estimate VLM in the proximity of glaciers. The Love numbers used in REAR are defined with respect to Earth's centre of mass (CM-frame).

The ongoing vertical adjustment caused by the melting of the large ice caps 21 Kyr ago is defined as GIA. We use the GIA-model from Caron et al. (2018), which uses 128000 forward models of different 1D Earth rheologies and ice elevation histories to create the statistical best fit to long term GNSS observations and relative sea level records from tide gauges. Even though GIA decays over time, the deacceleration is negligible for short time periods and thus the GIA-rate is assumed to be constant.

Both the elastic VLM-model and GIA is defined globally. However, the scope of this study is the wider Arctic area. This doesn't mean that the elastic VLM is negligible outside this region, but the VLM-signal from present-day ice-loss created VLM will not be significant.

2.1 Ice Loading

The main component of the elastic VLM model is the loading model. The elevation change rate for the ice areas included in this study is shown in figure S1.1 in S1 (Supporting Information). We only consider Northern Hemisphere ice history, well aware that also Southern Hemisphere ice mass change may impact the region of this study (Riva et al., 2017). However, mass loss of the Southern Hemisphere is considerably smaller and specifically Antarctica is so far away, that it safely can be neglected.

2.1.1 Glaciers

Included in this study are all glaciers from the Randolph Glacier Inventory (RGI 6.0) (Pfeffer et al., 2014; RGI Consortium, 2017) from North America, Russia, Scandinavia (incl. Svalbard) and Iceland - in total more than 62.000 individual glaciers. The mass loss from the glaciers included covers 95 % of the registered glacial mass loss in the Northern Hemisphere and constitute 80% of the global glacial mass loss (Zemp et al., 2019).

Mass change estimates for each glacier is derived by updating the model of Marzeion et al. (2012). Direct mass balance observations (Zemp et al., 2019) are used for calibration and validation of the glacier model. The glacier model translates information about atmospheric conditions into glacier mass change, taking into account various feedbacks between glacier mass balance and glacier geometry.

Glacial mass balance is combined with a distribution function, D to create glacier-wide surface elevation changes. This ensures, that the lower parts of the glacier is thinning, while the top is experiencing an small elevation gain. This 'slope steepening' of glaciers is a characteristic pattern for glaciers in many regions (Nuth et al., 2010; Foresta et al., 2016; Ciraci et al., 2018) and is assumed to all glaciers included in this study (see Supporting Information S1 for more detail on the glacier model).

2.1.2 Greenland

The glacial ice history is combined with elevation change from the Greenland Ice Sheet and adjoining glaciers. We estimate the rate of ice volume change from 2003–2015 by using altimeter surveys from NASA's ATM flights (Krabill, 2011) during 2003–2015 supplemented with high-resolution Ice, Cloud and land Elevation Satellite (ICESat) data

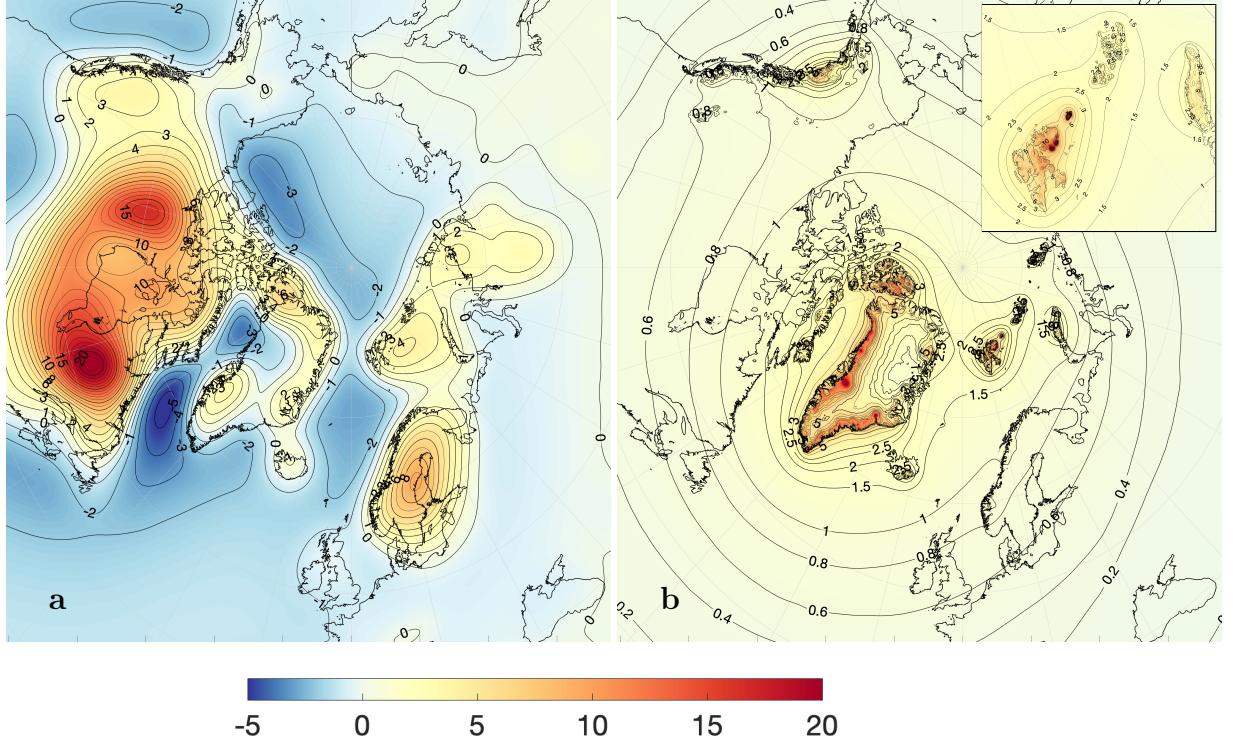


Figure 1. Average VLM rates (mm yr^{-1}) from 2003–2015 from Glacial Isostatic Adjustment (Caron et al., 2018) (a) and elastic rebound from contemporary land ice loss with enlargement of Svalbard (b).

(Zwally et al., 2011) during 2003–2009 and CryoSat-2 data during 2011–2015 (Helm et al., 2014). Our procedure for deriving ice surface elevation changes is described in detail by (Khan et al., 2013) and is similar to the method used by, e.g. Ewert et al. (2012); Smith et al. (2009) and Kjeldsen et al. (2013). We use the observed ice elevation change rates to interpolate (using collocation) ice thinning values onto the $2 \times 2 \text{ km}$ spatial grid. The volume loss rate is converted into a mass loss rate, taking firn compaction into account, as described by Kuipers Munneke et al. (2015).

2.2 GNSS data

Timeseries of vertical deformation and error estimates of 42 GNSS-sites are from the sixth release of the consortium lead by University of La Rochelle (ULR-6) (Santamaría-Gómez et al., 2017) (detailed map and timeseries of all glaciers are shown in S2 figure S2.1 and S3 figure S3.1). ULR-6 includes more than 80 GNSS-sites located in the area of interest, but we only select GNSS-sites with data in at least 120 of 156 months from 2003 to 2015 and where no known human impact is present. Furthermore, only one GNSS-site is selected based on the timeseries with the lowest standard deviation, when multiple GNSS-sites are located within 50 km of each other. The annual average is calculated for each GNSS-site and gaps are filled by assuming linearity. The trend estimates are calculated from the original time-series with outliers of more than $> 2\sigma$ removed.

3 Evaluating the VLM model

In figure 2, the VLM-model from 2003 to 2015, which is the sum of GIA and the modeled elastic VLM from figure 1, is shown together with VLM-rates from the GNSS sites described in section 2.2.

The model is dominated by the pattern of the GIA-model, with rates above 20 mm yr⁻¹ east of the Hudson Bay and another local maximum of over 15 mm yr⁻¹ in north-west Canada. The elastic rebound is evident, particular in Greenland with rates exceeding 10 mm yr⁻¹. Large areas around Svalbard and Alaska have modeled elastic VLM-rates of more than 6 mm yr⁻¹.

The largest rates of vertical deformations are areas dominated by elastic VLM. Jakobshavn Isbræ, north of Kangerlussuaq (KELY), has rates above 40 mm yr⁻¹. Similarly the area of Austfonna glacier on Svalbard has rates above 30 mm yr⁻¹. The largest depression zones are over the ocean, with the Beaufort Sea and Labrador Sea having rates below -2 mm yr⁻¹ and the Norwegian Sea with rates below -1.5 mm yr⁻¹. Subsiding coastal areas are found in North America, where Nova Scotia and most of the US east- and west-coast subsides with more than -1 mm yr⁻¹, while smaller subsidence (-0.5 - 0.0 mm yr⁻¹) is found in Northern Europe along the North Sea and Atlantic coastlines.

Figure 3 shows, that for large areas of the Arctic, the elastic VLM can be attributed with at least 30% from the VLM-signal. When GIA is small or zero, the elastic VLM is determining the vertical deformation. This is true for large areas in east Siberia and a band following around the North American east and west coast, as well as the northern part of the British Isles and the southern parts of Denmark and the Baltic Sea coast line.

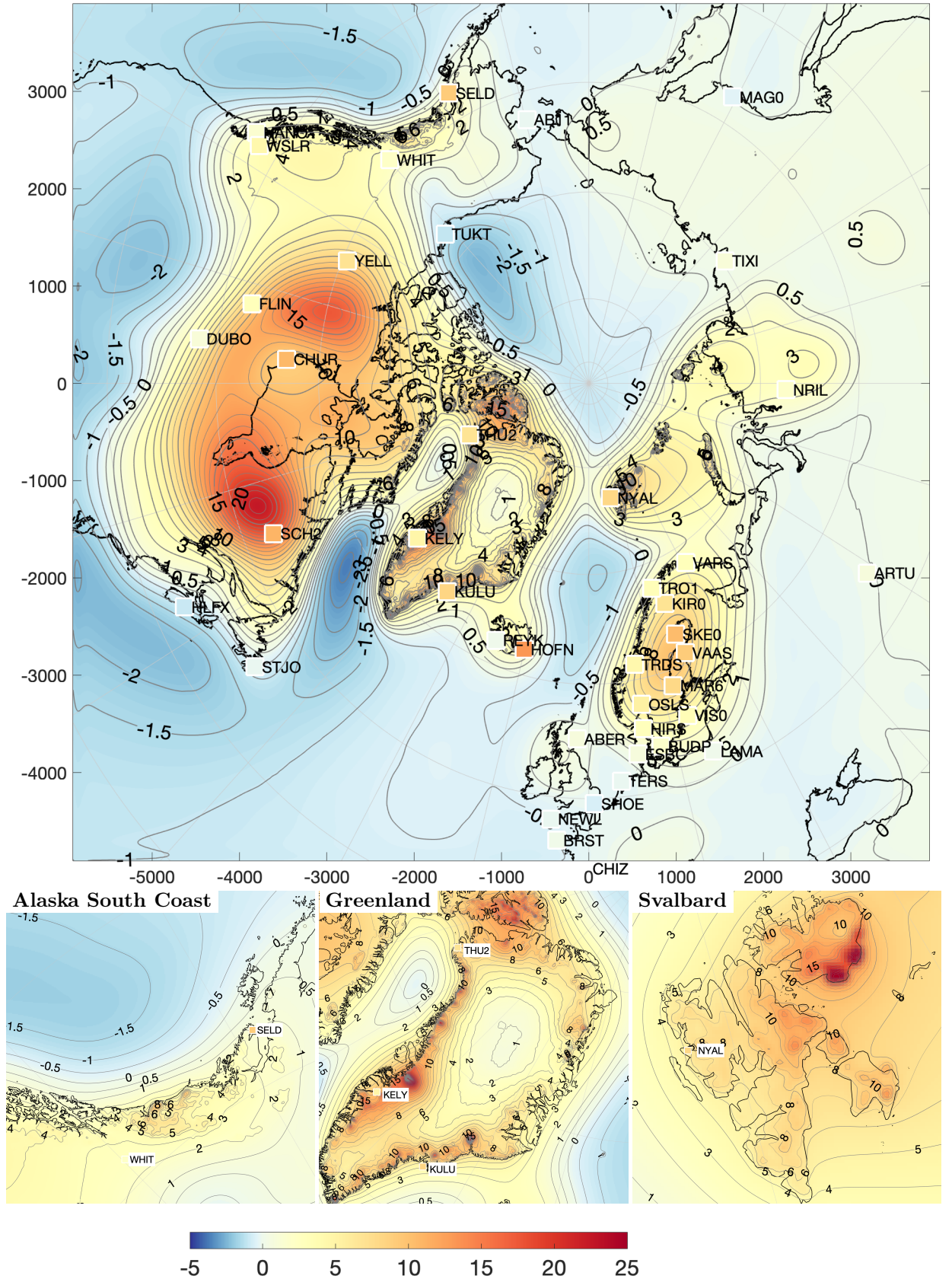


Figure 2. Average VLM-rates (mm yr⁻¹) from 2003-2015 from the VLM-model (Glacial Isostatic Adjustment + elastic VLM). The color of the squares represent the GNSS measured average VLM-rate for the same period. For clarification Alaska South Coast, Greenland and Svalbard are enlarged below.

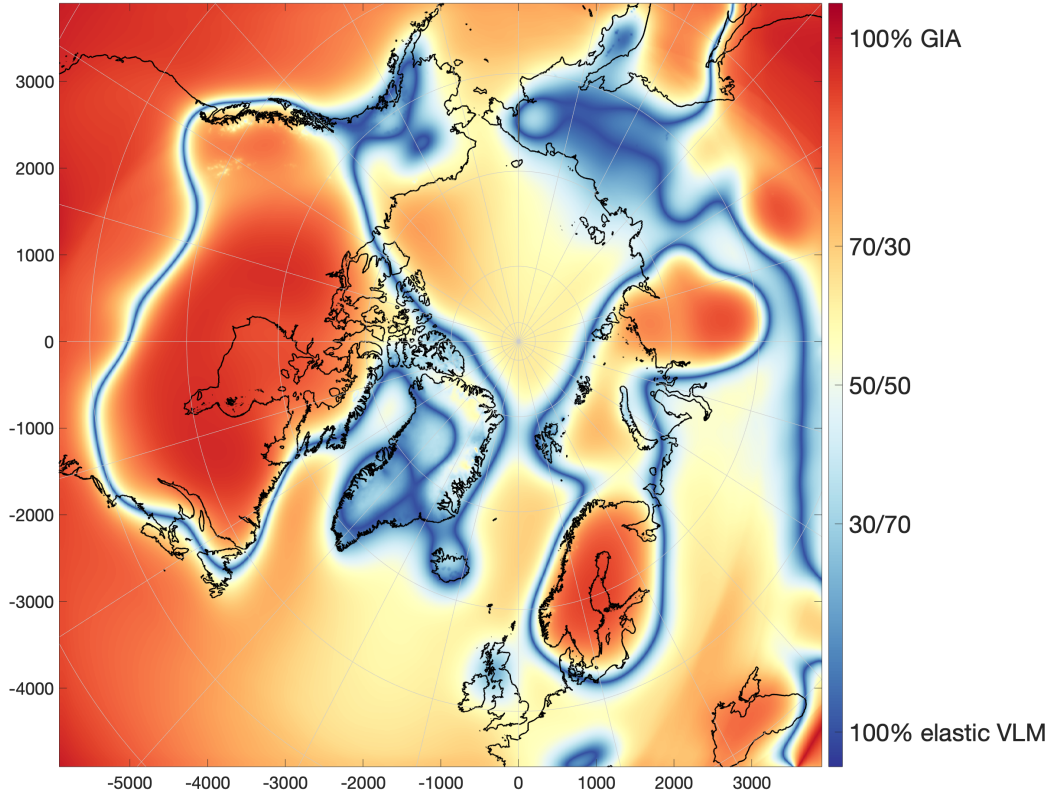


Figure 3. The share of GIA-rate and elastic VLM-rate from the total absolute VLM-rate (in absolute terms) in percentage. Red colors indicate areas where GIA dominates VLM while blue colors indicate where the elastic VLM is larger.

While the general uplift pattern from the VLM-model is reflected in the GNSS rates, residuals between GNSS VLM and the VLM model are evident, in particular close to glaciers. Figure 4 displays the difference between the VLM-model and the GNSS-measured VLM. The two largest differences are found in Seldovia, Alaska (SELD) and Hoefn, Iceland (HOFN). For Seldovia a large earthquake in 1964 is still causing displacement (Cohen & Freymueller, 2001), where on Iceland particular soft mantle structures creates larger uplift rates than predicted with the isotropic VLM-model (Fleming et al., 2007; Sørensen et al., 2017). The difference indicates the scale that extraordinary subsurface properties or post-seismic activities can have locally. More detailed information on local causes explaining the residuals in figure 4 are described in S2, table S2.1 and figure S3.1.

Some uncertainty is connected with the choice of GIA-model, for instance, the ICE6G-model from Peltier et al. (2015) has in other studies shown to provide a better fit to GNSS-sites in North America (Schumacher et al., 2018; Frederikse et al., 2019), where it seems that the Caron2018-model overestimates GIA slightly. In the early stages of this study, the Caron 2018 model provided the on average best fit to GNSS data compared to other GIA-models.

Figure 4 shows that the VLM-model including uncertainty is within the range of GNSS-measured VLM for 33 of the 42 GNSS locations. The correlation between measured VLM and GIA is 0.61, which improves to 0.74 when adding the elastic VLM to GIA (i.e. the VLM-model). The mean absolute error (MAE) of the 42 GNSS-sites is 1.54 mm yr^{-1} , which is 0.55 mm yr^{-1} better than a GIA-only model (2.09 mm yr^{-1}). If we don't consider sites located in glaciated areas (i.e. SELD, WHIT, THU2, KELY, KULU, REYK, HOFN, NYAL), then MAE becomes 0.89 mm yr^{-1} for the VLM-model which is significantly lower than 1.12 mm yr^{-1} for GIA-only.

When comparing to the associated barysteric sea level change of $\sim 1.4 \text{ mm yr}^{-1}$ (i.e. the ice loss created global average sea level change) is the elastic VLM significantly mitigating the sea level change at most GNSS-sites in this study (see figure 4)

The elastic VLM-rate is not linear, but unlike GIA, varies from year to year in accordance with the annual ice loss, as the elastic response is instant. This is in particular visible close to the ice loss, where the signal is largest and GNSS-measured VLM can be used as a proxy for the surrounding ice loss. Figure 5 shows how closely the VLM-model non linear follows the GNSS signal in Thule (THU2) in northern Greenland.

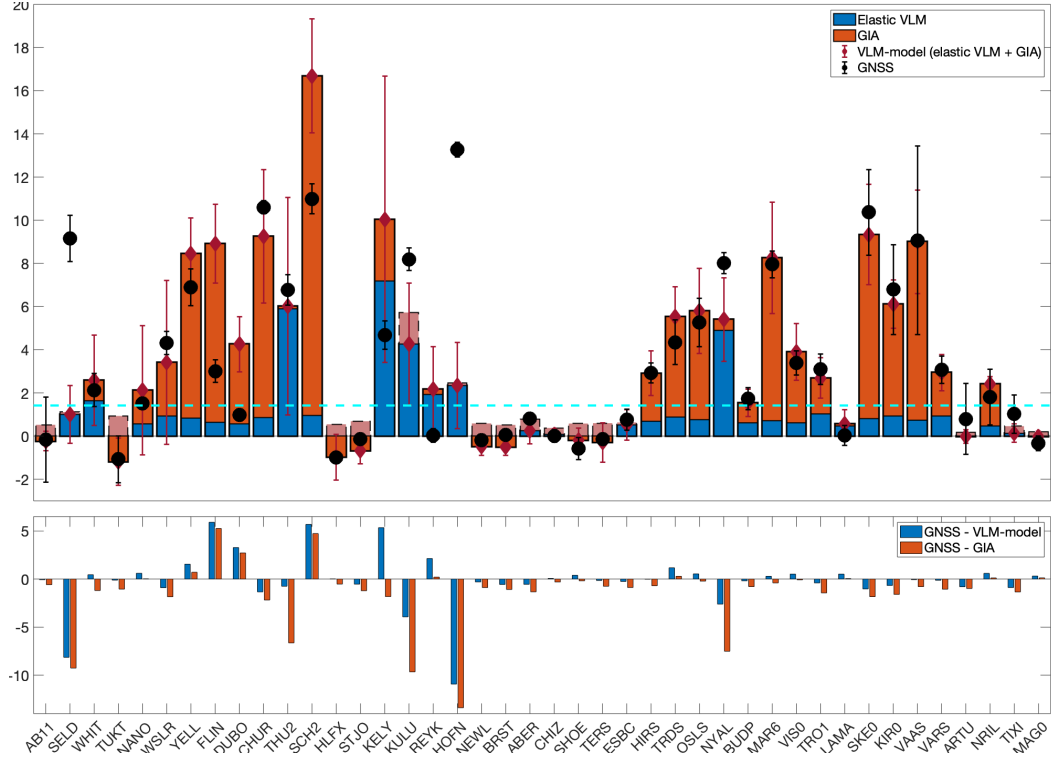


Figure 4. Top: 2003-2015 average VLM change [mm yr⁻¹] from the elastic VLM model (blue) and GIA (red) at 42 GNSS-sites shown in figure 2 and Supporting Information S2.1 ordered from most west (left) to most east (right). The dotted-cyan line indicates the average barysteric sea level rise (~ 1.4 mm yr⁻¹) from the ice loss included in this study. The total modeled VLM and the error is shown with red error bars and the GNSS measured VLM is shown with black error bars. The lighter red indicates where GIA is negative and hence overlaps the positive elastic VLM. Bottom: The residuals between GNSS-measured VLM and the VLM-model (blue) and GIA (red). The average of the absolute residuals (equivalent to Mean Absolute Error) is 1.54 mm yr⁻¹ and 2.09 mm yr⁻¹ respectively. All numbers for this figure are given in Supporting Information table S2.1.

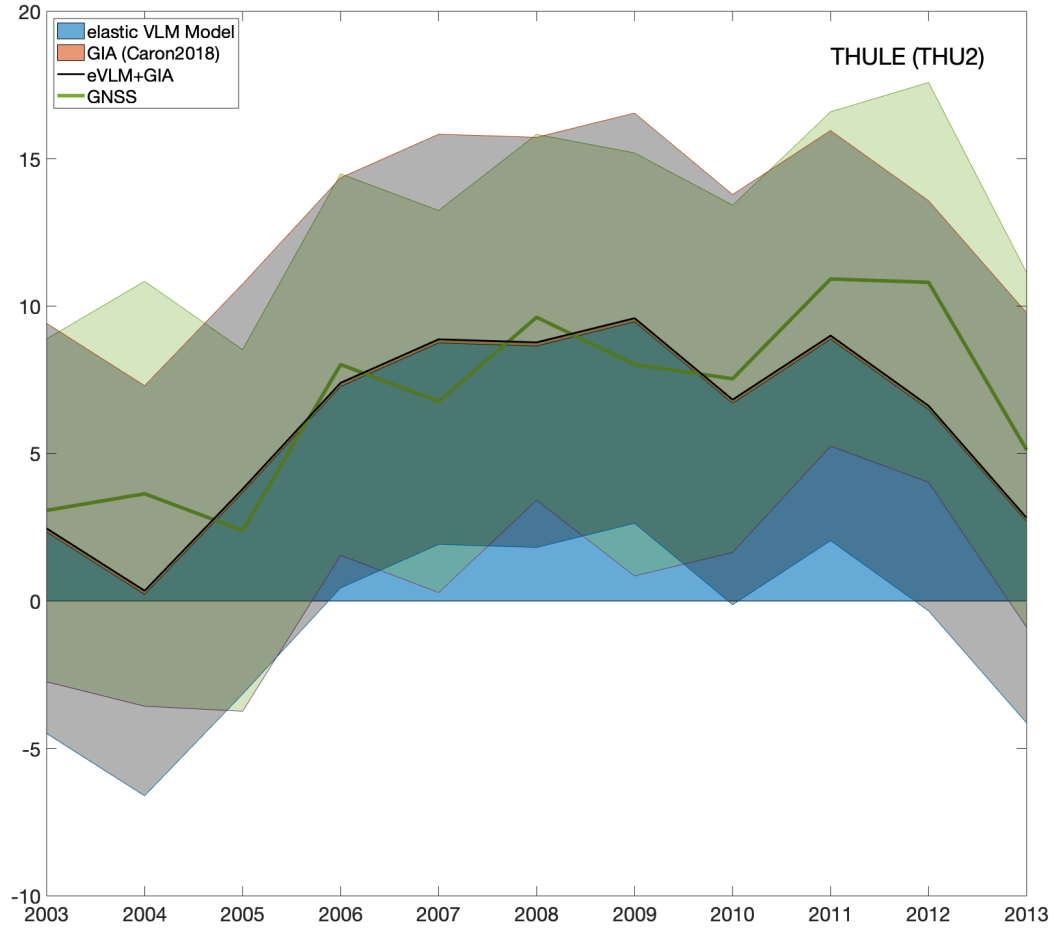


Figure 5. Yearly displacement (mm) for Thule (Northeast Greenland) from 2003 to 2013, measured by GNSS (green line - shaded green area is 1σ) and from the VLM-model (black line - shaded grey area is 1σ). The elastic VLM is represented by the blue area and GIA by the orange area, which in this case is small.

4 Discussion and Conclusion

Vertical Land Motion in the wider Arctic originates from many ongoing processes, with GIA and elastic VLM being the most important ones on regional to global scales. Even though this study is limited to an wider area around the Arctic, the VLM caused by changing cryosphere is a global effect (Riva et al., 2017; Kleinherenbrink et al., 2018; Frederikse et al., 2019).

By combining prehistoric (GIA) and present-day land ice change (elastic VLM), the VLM-model gives a realistic estimate on how the solid earth in the Arctic vertically deforms. By evaluating 42 selected GNSS-sites with a combined VLM-model, we find that the measured uplift by GNSS can be explained by either prehistoric or present-day land ice changes. For 33 of the GNSS-sites, the residual between GNSS measured VLM and the VLM-model is smaller than the associated errors.

The 2 x 2-km spatial resolution of the VLM-model is much higher than similar products from gravimetric satellite observations from GRACE (Adhikari et al., 2019). The spatial resolution improves the accuracy of VLM-predictions in glaciated regions, as local patterns of elastic deformation dominate the regional averages seen by GRACE (Frederikse et al., 2019). The VLM-model to GNSS comparison also indicates, that the VLM-model is inadequate in some regions due to local causes not covered by the VLM-model showing the scale of subsurface properties, past seismic activity or 19-20th century ice-loss (as seen on Svalbard (Mémin et al., 2014; Rajner, 2018)). A more detailed explanation of possible causes for differences between GNSS and the VLM is described in S2.

In non-glaciated areas, GNSS measurements have generally good agreement with the VLM-model. The contour lines in figure 1 shows that the elastic uplift is centered around Greenland, except close to other glaciated regions (e.g. Alaska and Svalbard), even though the total mass loss of the Arctic glaciers is comparable with the Greenland ice mass loss. Hence, the elastic uplift caused by Greenland ice melt is significant in the entire wider Arctic including the coastlines in Northern Europe and along the North American Atlantic.

Riva et al. (2017) showed, that the elastic uplift caused by Greenland eventually becomes negative in the Southern Hemisphere, which also means that Antarctica has a similar effect on the Northern Hemisphere. Antarctica experienced about half of the ice loss of Greenland during 2003-2015. However, we found that the Antarctic elastic VLM contribution is insignificant compared to that of the Northern Hemisphere and has uniform pattern for the region of this study. With potential future rapid ice loss (a.o. Edwards et al. (2019)), VLM caused by Antarctic ice loss will gain significance in the far field and hence be important to include for future coastal sea level projections in the Northern Hemisphere.

Acknowledgments

Thanks to Danielle Melini (Melini et al., 2014), for creating the REAR-code, which has been very helpful for creating the VLM-model. Greatly appreciated is the work of A. Caron (Caron et al., 2018) on the GIA-model, which is available from the NASA JPL website <https://ves1.jpl.nasa.gov/solid-earth/gia/>. The elastic VLM-model is freely available at <ftp.space.dtu.dk/pub/DTU20/VLM>. The project is partly funded by the EU-INTAROS project (Grant agreement 727890) and the ESA-Climate Change Initiative Sea level budget closure (Expro RFP/3-14679/16/I-NB).

References

Abram, N., Adler, C., Bindoff, N., Cheng, L., Cheong, S.-M., Cheung, W., ... Zhai, P. (2019, 09). Summary for policymakers. in: Ipcc special report on the ocean

- and cryosphere in a changing climate..
- Adhikari, S., Ivins, E. R., Frederikse, T., Landerer, F. W., & Caron, L. (2019). Sea-level fingerprints emergent from grace mission data. *Earth System Science Data*, 11(2), 629–646. Retrieved from <https://www.earth-syst-sci-data.net/11/629/2019/> doi: 10.5194/essd-11-629-2019
- Adhikari, S., Ivins, E. R., & Larour, E. (2016). Issm-sesaw v1.0: mesh-based computation of gravitationally consistent sea-level and geodetic signatures caused by cryosphere and climate driven mass change. *Geoscientific Model Development*, 9(3), 1087–1109. Retrieved from <https://www.geosci-model-dev.net/9/1087/2016/> doi: 10.5194/gmd-9-1087-2016
- Armitage, T. W. K., Manucharyan, G. E., Petty, A. A., Kwok, R., & Thompson, A. F. (2020). Enhanced eddy activity in the beaufort gyre in response to sea ice loss. *Nature Communications*, 11(1), 761. Retrieved from <https://doi.org/10.1038/s41467-020-14449-z> doi: 10.1038/s41467-020-14449-z
- Bamber, J., & Riva, R. (2010). The sea level fingerprint of recent ice mass fluxes. *The Cryosphere*, 4(4), 621–627. Retrieved from <https://www.the-cryosphere.net/4/621/2010/> doi: 10.5194/tc-4-621-2010
- Caron, L., Ivins, E. R., Larour, E., Adhikari, S., Nilsson, J., & Blewitt, G. (2018). Gia model statistics for grace hydrology, cryosphere, and ocean science. *Geophysical Research Letters*, 45(5), 2203–2212. Retrieved from <https://agupubs.onlinelibrary.wiley.com/doi/abs/10.1002/2017GL076644> doi: 10.1002/2017GL076644
- Church, J., & White, N. (2011). Sea-level rise from the late 19th to the early 21st century. *Surveys in Geophysics*, 32(4-5), 585–602. Retrieved from <https://www.scopus.com/inward/record.uri?eid=2-s2.0-80053195533&doi=10.1007%2fs10712-011-9119-1&partnerID=40&md5=a6a2b9bb53f622e9bf4b3266a27d54f0> (cited By 737) doi: 10.1007/s10712-011-9119-1
- Ciraci, E., Velicogna, I., & Sutterley, T. C. (2018). Mass balance of novaya zemlya archipelago, russian high arctic, using time-variable gravity from grace and altimetry data from icesat and cryosat-2. *Remote Sensing*, 10(11). Retrieved from <https://www.mdpi.com/2072-4292/10/11/1817> doi: 10.3390/rs10111817
- Cohen, S. C., & Freymueller, J. T. (2001). Crustal uplift in the south central alaska subduction zone: New analysis and interpretation of tide gauge observations. *Journal of Geophysical Research: Solid Earth*, 106(B6), 11259–11270. Retrieved from <https://agupubs.onlinelibrary.wiley.com/doi/abs/10.1029/2000JB900419> doi: 10.1029/2000JB900419
- Edwards, T., Brandon, M., Durand, G., Edwards, N., Gollledge, N., Holden, P., ... Wernecke, A. (2019, 02). Revisiting antarctic ice loss due to marine ice-cliff instability. *Nature*, 566, 58–64. doi: 10.1038/s41586-019-0901-4
- Ewert, H., Groh, A., & Dietrich, R. (2012, September). Volume and mass changes of the Greenland ice sheet inferred from ICESat and GRACE. *Journal of Geodynamics*, 59–60, 111–123. doi: 10.1016/j.jog.2011.06.003
- Farrell, W. E. (1972). Deformation of the earth by surface loads. *Reviews of Geophysics*, 10(3), 761–797. Retrieved from <https://agupubs.onlinelibrary.wiley.com/doi/abs/10.1029/RG010i003p00761> doi: 10.1029/RG010i003p00761
- Farrell, W. E., & Clark, J. A. (1976). On postglacial sea level. *Geophysical Journal of the Royal Astronomical Society*, 46(3), 647–667. Retrieved from <https://onlinelibrary.wiley.com/doi/abs/10.1111/j.1365-246X.1976.tb01252.x> doi: 10.1111/j.1365-246X.1976.tb01252.x
- Fleming, K., Martinec, Z., & Wolf, D. (2007, 01). Glacial-isostatic adjustment and the viscosity structure underlying the vatnajökull ice cap, iceland. *Pure and Applied Geophysics*, 164, 751–768. doi: 10.1007/s00024-007-0187-6

- 314 Foresta, L., Gourmelen, N., Pálsson, F., Nienow, P., Björnsson, H., & Shepherd, A.
315 (2016). Surface elevation change and mass balance of icelandic ice caps derived
316 from swath mode cryosat-2 altimetry. *Geophysical Research Letters*, 43(23),
317 12,138-12,145. Retrieved from [https://agupubs.onlinelibrary.wiley.com/](https://agupubs.onlinelibrary.wiley.com/doi/abs/10.1002/2016GL071485)
318 [doi/abs/10.1002/2016GL071485](https://doi.org/10.1002/2016GL071485) doi: 10.1002/2016GL071485
- 319 Frederikse, T., Landerer, F. W., & Caron, L. (2019). The imprints of contem-
320 porary mass redistribution on local sea level and vertical land motion ob-
321 servations. *Solid Earth*, 10(6), 1971–1987. Retrieved from [https://](https://www.solid-earth.net/10/1971/2019/)
322 www.solid-earth.net/10/1971/2019/ doi: 10.5194/se-10-1971-2019
- 323 Helm, V., Humbert, A., & Miller, H. (2014). Elevation and elevation change of
324 greenland and antarctica derived from cryosat-2. *The Cryosphere*, 8(4), 1539–
325 1559. Retrieved from <https://www.the-cryosphere.net/8/1539/2014/> doi:
326 10.5194/tc-8-1539-2014
- 327 Henry, O., Prandi, P., Llovel, W., Cazenave, A., Jevrejeva, S., Stammer, D., ...
328 Koldunov, N. (2012). Tide gauge-based sea level variations since 1950 along
329 the norwegian and russian coasts of the arctic ocean: Contribution of the steric
330 and mass components. *Journal of Geophysical Research: Oceans*, 117(C6).
331 Retrieved from [https://agupubs.onlinelibrary.wiley.com/doi/abs/](https://agupubs.onlinelibrary.wiley.com/doi/abs/10.1029/2011JC007706)
332 [10.1029/2011JC007706](https://doi.org/10.1029/2011JC007706) doi: 10.1029/2011JC007706
- 333 Hsu, C.-W., & Velicogna, I. (2017). Detection of sea level fingerprints derived
334 from grace gravity data. *Geophysical Research Letters*, 44(17), 8953-8961.
335 Retrieved from [https://agupubs.onlinelibrary.wiley.com/doi/abs/](https://agupubs.onlinelibrary.wiley.com/doi/abs/10.1002/2017GL074070)
336 [10.1002/2017GL074070](https://doi.org/10.1002/2017GL074070) doi: 10.1002/2017GL074070
- 337 Jevrejeva, S., Moore, J., Grinsted, A., Matthews, A., & Spada, G. (2014). Trends
338 and acceleration in global and regional sea levels since 1807. *Global and Plan-*
339 *etary Change*, 113, 11-22. Retrieved from [https://www.scopus.com/inward/](https://www.scopus.com/inward/record.uri?eid=2-s2.0-84890953576&doi=10.1016%2fj.gloplacha.2013.12.004&partnerID=40&md5=67194675f8fc061f1bb025a9fb67361f)
340 [record.uri?eid=2-s2.0-84890953576&doi=10.1016%2fj.gloplacha.2013](https://doi.org/10.1016/j.gloplacha.2013.12.004)
341 [.12.004&partnerID=40&md5=67194675f8fc061f1bb025a9fb67361f](https://doi.org/10.1016/j.gloplacha.2013.12.004) (cited By
342 85) doi: 10.1016/j.gloplacha.2013.12.004
- 343 Khan, S. A., Kjær, K. H., Korsgaard, N. J., Wahr, J., Joughin, I. R., Timm, L. H.,
344 ... Babonis, G. (2013). Recurring dynamically induced thinning during
345 1985 to 2010 on upernavik isstrøm, west greenland. *Journal of Geophys-*
346 *ical Research: Earth Surface*, 118(1), 111-121. Retrieved from [https://](https://agupubs.onlinelibrary.wiley.com/doi/abs/10.1029/2012JF002481)
347 agupubs.onlinelibrary.wiley.com/doi/abs/10.1029/2012JF002481 doi:
348 10.1029/2012JF002481
- 349 Khan, S. A., Liu, L., Wahr, J., Howat, I., Joughin, I., Dam, T. v., & Fleming,
350 K. (2010, 9). GPS measurements of crustal uplift near Jakobshavn Is-
351 bræ due to glacial ice mass loss. *Journal of Geophysical Research: Solid*
352 *Earth (1978–2012)*, 115(B9). Retrieved from [https://doi.org/10.1029/](https://doi.org/10.1029/2010JB007490)
353 [2010JB007490](https://doi.org/10.1029/2010JB007490) doi: 10.1029/2010JB007490
- 354 Khan, S. A., Sasgen, I., Bevis, M., van Dam, T., Bamber, J. L., Wahr, J., ...
355 Munneke, P. K. (2016). Geodetic measurements reveal similarities between
356 post-last glacial maximum and present-day mass loss from the greenland ice
357 sheet. *Science Advances*, 2(9). Retrieved from [https://advances.sciencemag](https://advances.sciencemag.org/content/2/9/e1600931)
358 [.org/content/2/9/e1600931](https://doi.org/10.1126/sciadv.1600931) doi: 10.1126/sciadv.1600931
- 359 Kjeldsen, K. K., Khan, S. A., Wahr, J., Korsgaard, N. J., Kjær, K. H., Bjørk, A. A.,
360 ... van Angelen, J. H. (2013). Improved ice loss estimate of the northwestern
361 greenland ice sheet. *Journal of Geophysical Research: Solid Earth*, 118(2),
362 698-708. Retrieved from [https://agupubs.onlinelibrary.wiley.com/doi/](https://agupubs.onlinelibrary.wiley.com/doi/abs/10.1029/2012JB009684)
363 [abs/10.1029/2012JB009684](https://doi.org/10.1029/2012JB009684) doi: 10.1029/2012JB009684
- 364 Kleinherenbrink, M., Riva, R., & Frederikse, T. (2018). A comparison of methods
365 to estimate vertical land motion trends from gnss and altimetry at tide gauge
366 stations. *Ocean Science*, 14(2), 187-204. Retrieved from [https://www.scopus](https://www.scopus.com/inward/record.uri?eid=2-s2.0-85044121271&doi=10.5194%2fos-14-187-2018&partnerID=40&md5=db85241ab9f3400fe3f655c42918079)
367 [.com/inward/record.uri?eid=2-s2.0-85044121271&doi=10.5194%2fos-14](https://doi.org/10.5194%2fos-14-187-2018&partnerID=40&md5=db85241ab9f3400fe3f655c42918079)
368 [-187-2018&partnerID=40&md5=db85241ab9f3400fe3f655c42918079](https://doi.org/10.5194%2fos-14-187-2018&partnerID=40&md5=db85241ab9f3400fe3f655c42918079) (cited

- By 6) doi: 10.5194/os-14-187-2018
- Klos, A., Kusche, J., Fenoglio-Marc, L., Bos, M. S., & Bogusz, J. (2019, Jul 24). Introducing a vertical land motion model for improving estimates of sea level rates derived from tide gauge records affected by earthquakes. *GPS Solutions*, 23(4), 102. Retrieved from <https://doi.org/10.1007/s10291-019-0896-1> doi: 10.1007/s10291-019-0896-1
- Krabill, W. B. (2011). *Icebridge atm l2 icesn elevation, slope, and roughness, [1993-2012]*. (Boulder, Colorado: NASA Distributed Active Archive Center at the National Snow and Ice Data Center) doi: 10.5067/ICESAT/GLAS/DATA225
- Kuipers Munneke, P., Ligtenberg, S. R. M., Noël, B. P. Y., Howat, I. M., Box, J. E., Mosley-Thompson, E., ... van den Broeke, M. R. (2015). Elevation change of the greenland ice sheet due to surface mass balance and firn processes, 1960-2014. *The Cryosphere*, 9(6), 2009–2025. Retrieved from <https://www.the-cryosphere.net/9/2009/2015/> doi: 10.5194/tc-9-2009-2015
- Ludwigsen, C. A., & Andersen, O. B. (2020). Contributions to arctic sea level from 2003 to 2015. *Advances in Space Research*. Retrieved from <http://www.sciencedirect.com/science/article/pii/S0273117719309275> doi: <https://doi.org/10.1016/j.asr.2019.12.027>
- Marzeion, B., Jarosch, A. H., & Hofer, M. (2012). Past and future sea-level change from the surface mass balance of glaciers. *The Cryosphere*, 6(6), 1295–1322. Retrieved from <https://www.the-cryosphere.net/6/1295/2012/> doi: 10.5194/tc-6-1295-2012
- Melini, D., Gegout, P., King, M., Marzeion, B., & Spada, G. (2015, 08). On the rebound: Modeling earth’s ever-changing shape. *Eos Transactions American Geophysical Union*, 96. doi: 10.1029/2015EO033387
- Melini, D., Spada, G., Gegout, P., & King, M. (2014, 01). *Rear - a regional elastic rebound calculator. user manual for version 1.0*. Retrieved from <http://hpc.rm.ingv.it/rear>
- Milne, G. A., & Mitrovica, J. X. (1998, 04). Postglacial sea-level change on a rotating Earth. *Geophysical Journal International*, 133(1), 1-19. Retrieved from <https://doi.org/10.1046/j.1365-246X.1998.1331455.x> doi: 10.1046/j.1365-246X.1998.1331455.x
- Nerem, R. S., Beckley, B. D., Fasullo, J. T., Hamlington, B. D., Masters, D., & Mitchum, G. T. (2018). Climate-change-driven accelerated sea-level rise detected in the altimeter era. *Proceedings of the National Academy of Sciences*, 115(9), 2022–2025. Retrieved from <https://www.pnas.org/content/115/9/2022> doi: 10.1073/pnas.1717312115
- Nuth, C., Moholdt, G., Kohler, J., Hagen, J. O., & Kääb, A. (2010). Svalbard glacier elevation changes and contribution to sea level rise. *Journal of Geophysical Research: Earth Surface*, 115(F1). Retrieved from <https://agupubs.onlinelibrary.wiley.com/doi/abs/10.1029/2008JF001223> doi: 10.1029/2008JF001223
- Peltier, W., Argus, D., & Drummond, R. (2015). Space geodesy constrains ice age terminal deglaciation: The global ice-6g-c (vm5a) model. *Journal of Geophysical Research: Solid Earth*, 120(1), 450-487. Retrieved from <https://www.scopus.com/inward/record.uri?eid=2-s2.0-85027948080&doi=10.1002%2f2014JB011176&partnerID=40&md5=29a7ce38c5cf3872d2276981d2f6b34f> (cited By 326) doi: 10.1002/2014JB011176
- Pfeffer, W. T., Arendt, A. A., Bliss, A., Bolch, T., Cogley, J. G., Gardner, A. S., ... et al. (2014). The randolph glacier inventory: a globally complete inventory of glaciers. *Journal of Glaciology*, 60(221), 537–552. doi: 10.3189/2014JoG13J176
- Post, E., Alley, R. B., Christensen, T. R., Macias-Fauria, M., Forbes, B. C., Gooseff, M. N., ... Wang, M. (2019). The polar regions in a 2c warmer world. *Science Advances*, 5(12). Retrieved from <https://advances.sciencemag.org/>

- content/5/12/eaaw9883 doi: 10.1126/sciadv.aaw9883
- RGI Consortium. (2017). *Randolph Glacier Inventory – A Dataset of Global Glacier Outlines: Version 6.0: Technical Report*. (<https://doi.org/10.7265/N5-RGI-60>)
- Riva, E., Frederikse, T., King, A., Marzeion, B., & Van Den Broeke, R. (2017). Brief communication: The global signature of post-1900 land ice wastage on vertical land motion. *Cryosphere*, 11(3), 1327-1332. Retrieved from <https://www.scopus.com/inward/record.uri?eid=2-s2.0-85020484420&doi=10.5194/2ftc-11-1327-2017&partnerID=40&md5=077251aec38900cef0ec0ecdd2b1eded> (cited By 11) doi: 10.5194/2ftc-11-1327-2017
- Santamaría-Gómez, A., Gravelle, M., Dangendorf, S., Marcos, M., Spada, G., & Wöppelmann, G. (2017). Uncertainty of the 20th century sea-level rise due to vertical land motion errors. *Earth and Planetary Science Letters*, 473, 24 - 32. Retrieved from <http://www.sciencedirect.com/science/article/pii/S0012821X17303060> doi: <https://doi.org/10.1016/j.epsl.2017.05.038>
- Schumacher, M., King, M., Rougier, J., Sha, Z., Khan, S., & Bamber, J. (2018). A new global gps data set for testing and improving modelled glacial uplift rates. *Geophysical Journal International*, 214(3), 2164-2176. Retrieved from <https://www.scopus.com/inward/record.uri?eid=2-s2.0-85050475763&doi=10.1093%2fgji%2fggy235&partnerID=40&md5=0b6d3ed0cdf0208346d1d8bb4bed2c40> (cited By 5) doi: 10.1093/gji/ggy235
- Smith, B. E., Fricker, H. A., Joughin, I. R., & Tulaczyk, S. (2009). An inventory of active subglacial lakes in Antarctica detected by ICESat (2003–2008). *Journal of Glaciology*, 55(192), 573–595. doi: 10.3189/002214309789470879
- Sørensen, L. S., Jarosch, A. H., Adalgeirsdóttir, G., Barletta, V. R., Forsberg, R., Pálsson, F., ... Jóhannesson, T. (2017, 01). The effect of signal leakage and glacial isostatic rebound on GRACE-derived ice mass changes in Iceland. *Geophysical Journal International*, 209(1), 226-233. Retrieved from <https://doi.org/10.1093/gji/ggx008> doi: 10.1093/gji/ggx008
- Tushingham, A. M., & Peltier, W. R. (1991). Ice-3g: A new global model of late Pleistocene deglaciation based upon geophysical predictions of post-glacial relative sea level change. *Journal of Geophysical Research: Solid Earth*, 96(B3), 4497-4523. Retrieved from <https://agupubs.onlinelibrary.wiley.com/doi/abs/10.1029/90JB01583> doi: 10.1029/90JB01583
- Watson, C. S., White, N. J., Church, J. A., King, M. A., Burgette, R. J., & Legresy, B. (2015, JUN). Unabated global mean sea-level rise over the satellite altimetry era. *NATURE CLIMATE CHANGE*, 5(6), 565+.
- Wöppelmann, G., & Marcos, M. (2016). Vertical land motion as a key to understanding sea level change and variability. *Reviews of Geophysics*, 54(1), 64-92. Retrieved from <https://agupubs.onlinelibrary.wiley.com/doi/abs/10.1002/2015RG000502> doi: 10.1002/2015RG000502
- Zemp, M., Huss, M., Thibert, E., Eckert, N., McNabb, R., Huber, J., ... Cogley, J. G. (2019). Global glacier mass changes and their contributions to sea-level rise from 1961 to 2016. *Nature*, 568(7752), 382-386. doi: 10.1038/s41586-019-1071-0
- Zwally, H. J., Schutz, R., Bentley, C., Bufton, J., Herring, T., Minster, J., ... Thomas, R. (2011). *Glas/icesat l2 antarctic and greenland ice sheet altimetry data v031*. (Boulder, Colorado: NASA Distributed Active Archive Center at the National Snow and Ice Data Center) doi: 10.5067/CPRXXK3F39RV

References of Supporting Information:

- Caron, L., Ivins, E. R., Larour, E., Adhikari, S., Nilsson, J., & Blewitt, G. (2018). GIA model statistics for GRACE hydrology, cryosphere, and ocean science. *Geo-*

- physical Research Letters, 45(5), 2203-2212. Retrieved from <https://agupubs.onlinelibrary.wiley.com/doi/abs/10.1002/2017GL076644> doi: 10.1002/2017GL076644
- Cohen, S. C., & Freymueller, J. T. (2001). Crustal uplift in the south central alaska subduction zone: New analysis and interpretation of tide gauge observations. *Journal of Geophysical Research: Solid Earth*, 106(B6), 11259-11270. Retrieved from <https://agupubs.onlinelibrary.wiley.com/doi/abs/10.1029/2000JB900419> doi: 10.1029/2000JB900419
- Fleming, K., Martinec, Z., & Wolf, D. (2007, 01). Glacial-isostatic adjustment and the viscosity structure underlying the vatnajökull ice cap, iceland. *Pure and Applied Geophysics*, 164, 751-768. doi: 10.1007/s00024-007-0187-6
- Frederikse, T., Landerer, F. W., & Caron, L. (2019). The imprints of contemporary mass redistribution on local sea level and vertical land motion observations. *Solid Earth*, 10(6), 1971-1987. Retrieved from <https://www.solid-earth.net/10/1971/2019/> doi: 10.5194/se-10-1971-2019
- Grove, J. (2001, 01). The initiation of the "little ice age" in regions round the north atlantic. *Climatic Change*, 48, 53-82. doi: 10.1023/A:1005662822136
- Hu, Y., & Freymueller, J. T. (2019). Geodetic observations of time-variable glacial isostatic adjustment in southeast alaska and its implications for earth rheology. *Journal of Geophysical Research: Solid Earth*, 124(9), 9870-9889. Retrieved from <https://agupubs.onlinelibrary.wiley.com/doi/abs/10.1029/2018JB017028> doi: 10.1029/2018JB017028
- Kierulf, H. P., Plag, H.-P., & Kohler, J. (2009, 10). Surface deformation induced by present-day ice melting in Svalbard. *Geophysical Journal International*, 179(1), 1-13. Retrieved from <https://doi.org/10.1111/j.1365-246X.2009.04322.x> doi: 10.1111/j.1365-246X.2009.04322.x
- Larsen, C. F., Motyka, R. J., Freymueller, J. T., Echelmeyer, K. A., & Ivins, E. R. (2005). Rapid viscoelastic uplift in southeast alaska caused by post-little ice age glacial retreat. *Earth and Planetary Science Letters*, 237(3), 548 - 560. Retrieved from <http://www.sciencedirect.com/science/article/pii/S0012821X05004152> doi: <https://doi.org/10.1016/j.epsl.2005.06.032>
- Mémin, A., Spada, G., Boy, J.-P., Rogister, Y., & Hinderer, J. (2014, 05). Decadal geodetic variations in Ny-Ålesund (Svalbard): role of past and present ice-mass changes. *Geophysical Journal International*, 198(1), 285-297. Retrieved from <https://doi.org/10.1093/gji/ggu134> doi: 10.1093/gji/ggu134
- Peltier, W., Argus, D., & Drummond, R. (2015). Space geodesy constrains ice age terminal deglaciation: The global ice-6g-c (vm5a) model. *Journal of Geophysical Research: Solid Earth*, 120(1), 450-487. Retrieved from <https://www.scopus.com/inward/record.uri?eid=2-s2.0-85027948080&doi=10.1002/2f2014JB011176&partnerID=40&md5=29a7ce38c5cf3872d2276981d2f6b34f> (cited By 326) doi: 10.1002/2014JB011176
- Pfeffer, W. T., Arendt, A. A., Bliss, A., Bolch, T., Cogley, J. G., Gardner, A. S., ... et al. (2014). The randolph glacier inventory: a globally complete inventory of glaciers. *Journal of Glaciology*, 60(221), 537-552. doi: 10.3189/2014JoG13J176
- Rajner, M. (2018). Detection of ice mass variation using gnss measurements at svalbard. *Journal of Geodynamics*, 121, 20 - 25. Retrieved from <http://www.sciencedirect.com/science/article/pii/S0264370718300450> doi: <https://doi.org/10.1016/j.jog.2018.06.001>
- Root, B. C., Tarasov, L., & van der Wal, W. (2015). Grace gravity observations constrain weichselian ice thickness in the barents sea. *Geophysical Research Letters*, 42(9), 3313-3320. Retrieved from <https://agupubs.onlinelibrary.wiley.com/doi/abs/10.1002/2015GL063769> doi: 10.1002/2015GL063769
- Sato, T., Okuno, J., Hinderer, J., MacMillan, D. S., Plag, H.-P., Francis, O., ... Fukuda, Y. (2006, 06). A geophysical interpretation of the secular displace-

532 ment and gravity rates observed at Ny-Ålesund, Svalbard in the Arctic—effects
 533 of post-glacial rebound and present-day ice melting. *Geophysical Journal In-*
 534 *ternational*, 165(3), 729-743. Retrieved from [https://doi.org/10.1111/](https://doi.org/10.1111/j.1365-246X.2006.02992.x)
 535 [j.1365-246X.2006.02992.x](https://doi.org/10.1111/j.1365-246X.2006.02992.x) doi: 10.1111/j.1365-246X.2006.02992.x
 536 Sørensen, L. S., Jarosch, A. H., Adalgeirsdóttir, G., Barletta, V. R., Forsberg, R.,
 537 Pálsson, F., ... Jóhannesson, T. (2017, 01). The effect of signal leakage
 538 and glacial isostatic rebound on GRACE-derived ice mass changes in Ice-
 539 land. *Geophysical Journal International*, 209(1), 226-233. Retrieved from
 540 <https://doi.org/10.1093/gji/ggx008> doi: 10.1093/gji/ggx008
 541 Tushingham, A. M., & Peltier, W. R. (1991). Ice-3g: A new global model of late
 542 pleistocene deglaciation based upon geophysical predictions of post-glacial rel-
 543 ative sea level change. *Journal of Geophysical Research: Solid Earth*, 96(B3),
 544 4497-4523. Retrieved from [https://agupubs.onlinelibrary.wiley.com/](https://agupubs.onlinelibrary.wiley.com/doi/abs/10.1029/90JB01583)
 545 [doi/abs/10.1029/90JB01583](https://agupubs.onlinelibrary.wiley.com/doi/abs/10.1029/90JB01583) doi: 10.1029/90JB01583
 546 VanLooy, J., Forster, R., & Ford, A. (2006). Accelerating thinning of kenai
 547 peninsula glaciers, alaska. *Geophysical Research Letters*, 33(21). Retrieved
 548 from [https://agupubs.onlinelibrary.wiley.com/doi/abs/10.1029/](https://agupubs.onlinelibrary.wiley.com/doi/abs/10.1029/2006GL028060)
 549 [2006GL028060](https://agupubs.onlinelibrary.wiley.com/doi/abs/10.1029/2006GL028060) doi: 10.1029/2006GL028060
 550 Whitehouse, P. L., Allen, M. B., & Milne, G. A. (2007, 08). Glacial isostatic ad-
 551 justment as a control on coastal processes: An example from the Siberian
 552 Arctic. *Geology*, 35(8), 747-750. Retrieved from [https://doi.org/10.1130/](https://doi.org/10.1130/G23437A.1)
 553 [G23437A.1](https://doi.org/10.1130/G23437A.1) doi: 10.1130/G23437A.1